Polypropylene nanocomposites produced by in-situ grafting of n-butyl acrylate

Journal:	*Journal of Applied Polymer Science*
Manuscript ID:	APP-2015-03-0776.R1
Wiley - Manuscript type:	Research Article
Keywords:	polyolefins, nanostructured polymers, grafting, clay

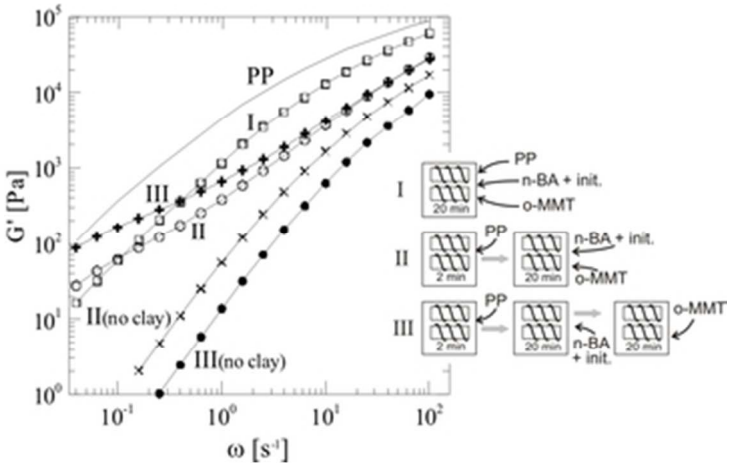

30x19mm (300 x 300 DPI)

Polypropylene Nanocomposites produced by in-situ grafting of n-butyl acrylate

Julie Merchán Sandoval[1], Lidia M. Quinzani[1], Marcelo D. Failla[1,2,*]

[1] Planta Piloto de Ingeniería Química (PLAPIQUI), UNS-CONICET - C.C. 717 - Bahía Blanca 8000, Argentina

[2] Departamento de Ingeniería, Universidad Nacional del Sur (UNS), Av. Alem 1253 - Bahía Blanca 8000, Argentina

[*] Corresponding author: mfailla@plapiqui.edu.ar - FAX (54) 291-4861600

Keywords: Nanocomposites, Polypropylene, In-situ functionalization, Montmorillonite, n-butyl acrylate, Thermal properties, Rheological properties

Abstract

Nanocomposites of polypropylene and organophilic clay are produced by *in situ* functionalization of PP with n-butyl acrylate (BA) during melt mixing. Three strategies for incorporating materials into the mixer are analyzed and the effect of clay concentration is evaluated. The materials are examined by FTIR spectroscopy, X-ray diffraction, scanning electron microscopy, differential scanning calorimetry, thermogravimetry and rotational reometry. The results show that all composites prepared in the presence of BA have similar intercalated clay structure, and that the largest degree of exfoliation is obtained using the sequential mixing technique. This method, which consists in adding the initiator and functionalizing agent to the molten polypropylene followed by the addition of the clay, also produces the largest reduction in molecular weight of the polymer and the largest increase of the elastic modulus. All polymers show similar crystallization and degradation processes.

INTRODUCTION

Polypropylene (PP) is one of the most consumed polyolefins due to its adequate performance-cost balance and good properties. Moreover, PP admits several ways of enhance and/or modify its properties to expand its application range. One way to modify PP is through the addition of low concentrations of nano-fillers. The presence of fillers that have at least one dimension in the nano-scale range should improve the physical and mechanical properties of raw materials with a small change of specific gravity and optical properties.[1-2]

One of the most frequently used nano-fillers in the preparation of PP nanocomposites is montmorillonite (MMT). This is a stratified clay that belongs to the smectite group.[3] However, the chemical composition of this clay makes it non-compatible with polyolefins. To overcome this disadvantage and reduce the superficial energy to give the clay surface a more hydrophobic character, MMT is usually modified by cation exchange. This treatment typically consists in exchanging the small inorganic cations that naturally appear on the surface of the clay layers by alkylamonium cations with long alkyl chains. These molecules increase the distance between clay platelets and facilitate the future distribution and delamination of the clay in the polymer matrix during processing.

At least three methods are used to process nanocomposites: in-situ polymerization, solution mixing and melt mixing.[2] The last one is normally employed in the case of polyolefins because it can be easily applied using current industrial transforming equipment and has low environmental impact. However, the low affinity between PP and MMT, even the organophilic one (o-MMT), makes it necessary to include a compatibilizer to achieve a reasonable dispersion of the clay when using processing in the molten state. The most used compatibilizers are PP functionalized with polar groups like anhydrides, acrylates, acids, etc. In that sense, maleated PP is the compatibilizer most frequently used.[4-10]

Although the use of low concentrations of a compatibilizer is the most used scheme among melt mixing methods, various other strategies of compatibilization between inorganic loadings and PP have been reported. For example, pretreatment of the loading with coupling agents;[11-13] generation of radicals which react with both, the PP free radicals generated during processing and with the loading via, for example, electron transferring;[14] incorporation of monomers which undergo grafting onto PP during processing using a peroxide to initiate the grafting,[15-17] etc. In particular, the in-situ functionalization of PP during blending with o-MMT is an interesting alternative among melt mixing methods since it is easily implemented in current industrial processes and may promote clay exfoliation. Moreover, this is a method that may achieve better compatibility between PP and functionalized PP molecules than the

physical melt mixing of PP and a pre-functionalized PP. However, one limitation of the modification of PP in the presence of organic peroxides is the occurrence of chain scission and consequent decrease of PP molecular weight.

Lin and coworkers[15] prepared composites based on PP, nano-$CaCO_3$ treated with stearic acid and acrylic acid (AA), with and without dicumyl peroxide (DCP) using a twin-screw extruder. They found that the crystallization temperature (T_c) of PP slightly decreases when 2 and 5wt% of filler are added but it increases for 10 and 40wt%. They suggest that the nano-$CaCO_3$ only has a nucleating effect at large concentrations because only then the filler losses its coating of stearic acid during mixing. The addition of AA to PP in the presence of 40wt% of nano-$CaCO_3$ reduces the T_c, which then increases with AA content. The authors propose that this occurs because of the formation of $Ca(AA)_2$ which promotes the nucleation of PP. The presence of the peroxide reverses this behavior. That is, the addition of AA to PP in the presence of 40wt% of filler and DCP increases the T_c, which then decreases with AA content. The competing effects of the formation of PP grafted with AA and of $Ca(AA)_2$ may explain this behavior.

Zhang *et al*.[16] synthesized PP–clay nanocomposites by in situ grafting-intercalation in the molten state following three main steps. First, they modified the o-MMT with maleic anhydride (MA) in solution with a small amount of a co-swelling agent and the initiator. Then, they melt-mixed the impregnated clay with PP in a laboratory mixer at 180°C to obtain a masterbatch; and finally, they blended PP with different amounts of masterbatch at 190°C to obtain composites with 1 to 4wt% of o-MMT. The results suggest that the clay is partially exfoliated in the masterbatch and fully exfoliated in the nanocomposites, and that the materials have improved thermal stability and stiffness.

Passaglia and coworkers[17] used a similar approach to synthesize nanocomposites based in four different ethylene/propylene copolymers, two functionalizing agents (MA and diethyl maleate) and one o-MMT. They also compare the results from using three melt mixing procedures: one in which the polymer was functionalized and then mixed with the organoclay; another in which the polymer was introduced in the mixer chamber followed by a slurry of peroxide/functionalizing agent/o-MMT that was added 2 min later; and a third one in which the polymer was introduced in the mixer chamber followed by a peroxide/functionalizing agent mixture that was added 2 min later and the o-MMT that was introduced a few more minutes later. The results from this work, which are associated to a very large amount of variables, mainly indicate the complexity of the process in terms of the role played by the different parameters, including the polymer chemical structure. According to the authors, in

the case of the copolymer with low ethylene content, the application of the three-step method seems to favor the functionalization of PP and to achieve a better dispersion of the clay particles. Moreover, they observe that the largest degree of intercalation was obtained when the degradation was significant during the functionalization process, indicating that the reduction of molecular weight was probably even more effective than the presence of a larger amount of grafted polar groups.

The three previous studies are the only references that were found in the literature dealing with the grafting of PP or propylene-ethylene copolymer during mixing with the nanofiller. None of them consider a one step process of in-situ functionalization of PP with o-MMT, which is the most useful method from the industrial point of view to obtain PP nanocomposites. In the present work, nanocomposites of PP and o-MMT have been prepared by in-situ functionalization of the polymer during melt mixing. The chosen functionalizing agent is n-butyl acrylate (BA). To our knowledge, the BA has not been previously used to functionalize PP in the preparation of nanocomposites, not even to use the BA-grafted PP as compatibilizer, although a few authors have consider the grafting of BA onto powdered PP[18-20] and even fewer have analyzed the grafting in solution.[21] The BA, which is easier to handle than MA and is less corrosive, may promote compatibility of the polymer with the clay and the clay modifier. The aim of this work is to obtain nanocomposites of PP and o-MMT by in-situ grafting of a BA in a one step melt reactive processing. For this, different procedures of nanocomposite preparation are compared through the analysis of the morphological, thermal and rheological characteristics of the synthesized composites.

EXPERIMENTAL

Materials

The polymer used to prepare the composites is a commercially available isotactic PP supplied by *Petroquímica Cuyo SAIC* (M_w = 330 kg/mol, M_w/M_n = 4.7). The organophilic clay is a commercial MMT (*Nanomer I.44P*, from *Nanocor*) that has been modified with dimethyl-dihydrogenated-tallow ammonium chloride. This clay has particle size in the range 15-25 μm, a modifier concentration of 1.04 meq/g of inorganic clay with surface coverage of about 70%, a decomposition temperature of 200°C, and 2.6 nm of interlayer spacing.[9] The n-butyl acrylate (BA, *Sigma Aldrich*) and the 2,5-dimethyl-2,5-di(tert-butyl peroxy)hexane (DBPH, *Akzo Nobel*) were used as provided.

Preparation of composites

All polymeric materials, even the PP, were processed at 180°C in a *Brabender Plasto-graph*® mixer using 20 rpm and nitrogen atmosphere. Three different mixing procedures, which are summarized in Table 1, were used to prepare the composites. The concentrations of BA and DBPH considered in this work are 1 and 0.075wt% respectively, based on PP mass, while three values of clay concentration were used: 2, 5 and 10wt%. These values correspond to 1.94, 4.71 and 9.00 wt% based on composites. A small amount (0.045 g) of Irganox 1010 was added to all processed materials a couple of minutes before the end of the mixing process. After mixing, the materials were removed from the mixer chamber with a spatula and compressed between aluminum plates to obtain approximately 2 mm thick samples.

Table 1. Mixing procedures used to prepare the nanocomposites.

Method	Description
I	Step 1: clay is impregnated with BA Step 2: PP, impregnated clay, and DBPH are physically mixed together Step 3: the mix is added into the mixer at 180°C and processed during 20 min
II	Step 1: PP is melted in the mixer at 180°C (approx. 2 min) Step 2: DBPH, BA and the clay are added into the mixer and processed during 20 min
III	Step 1: PP is melted in the mixer at 180°C (approx. 2 min) Step 2: DBPH and BA are simultaneously added to PP and processed during 20 min Step 3: clay is incorporated and processed 20 min more

Table 2 lists all the synthesized materials: seven composites and five polymeric systems were prepared for comparison. The composites are identified as NB*xy*, where *x* is a number that represents the weight percentage of o-MMT and *y* is a roman number associated to the mixing procedure. The rest are: two functionalized PP (PPBII and PPBIII), a PP modified only with peroxide (PPp), and two composites that were prepared without functionalizing agent (N10II and N10III).

Characterization

Infrared spectra of all materials were recorded using a *Nicolet 520* FTIR spectrophotometer with a resolution of 4 cm^{-1}. The spectra were obtained on ~30 μm thick films that were previously prepared by compression molding at 190°C using purified materials. The purification consisted in dissolving the polymeric systems in xylene at 135°C under constant stirring and nitrogen atmosphere, and then precipitating them using cold methyl-ethyl-ketone. The precipitates were dried at 80°C for 48 h under vacuum.

Table 2. List of materials synthesized and basal spacing of MMT

	peroxide [1] (wt%)	BA [1] (wt%)	o-MMT [1] (wt%)	Method	mixing time (min)	d_{001} of MMT (nm)
PP	- - -	- - -	- - -	- - -	20	- - -
PPp	0.075	- - -	- - -	~ I [2]	20	- - -
PPBII	0.075	1	- - -	~ II [2]	20	- - -
PPBIII	0.075	1	- - -	~ III [2]	40	- - -
NB10I	0.075	1	10	I	20	3.4
NB2II	0.075	1	2	II	20	- - -
NB5II	0.075	1	5	II	20	3.6
NB10II	0.075	1	10	II	20	3.5
N10II	0.075	- - -	10	II	20	- - -
NB2III	0.075	1	2	III	40	3.7
NB5III	0.075	1	5	III	40	3.5
NB10III	0.075	1	10	III	40	3.5
N10III	0.075	- - -	10	III	40	- - -

[1] nominal values based on PP mass

[2] refers to order of incorporation of components and mixing time, even if there is no clay present

X-ray diffraction (XRD) was used to analyze the structure of the materials and to determine the interlayer spacing between stacked clay platelets. The study was done using a *Phillips PW1710* X-ray diffractometer equipped with a Cu Kα radiation source of wavelength 1.54 Å operated at 45 kV and 30 mA. The diffraction spectra were recorded in the reflection mode over a 2θ range of 2-40° in steps of 0.020° using a rate of 0.6°/min. The clay powder and 2 mm thick polymeric samples were characterized with this technique. The PNC samples were previously slightly compress-molded at 180°C for 3 minutes to produce smooth and flat surfaces. To complete the structural characterization of the materials, the morphology of the composites was observed by scanning electronic microscopy (SEM) using a *LEO EVO-40 XVP* equipment.

The rheological characterization was performed using small-amplitude oscillatory shear flow in an *AR-G2* system from *TA Instruments* equipped with 25 mm diameter plates. The dynamic moduli were registered at 180°C under stress-controlled mode using frequency sweep tests between 0.04 and 100 s^{-1}. The constant shear stress was selected to guaranty that the measurements correspond to the linear viscoelastic regime. Three samples of each material were tested, always using nitrogen atmosphere.

The crystallization and fusion processes of all materials was analyzed by differential scanning calorimetry (DSC) using a *Pyris 1* calorimeter from *Perkin Elmer*. Samples of about 8 mg were heated up to 200°C under nitrogen atmosphere and held at this temperature for 5 min to erase the thermal history. Then, they were cooled up to 30°C and heated back to 200°C at a rate of 10°C/min. Three samples of each material were tested and the results averaged.

To complete the thermal analysis, the stability of the polymeric systems was studied by thermogravimetry (TGA) using a *Discovery* system from *TA Instruments*. The samples were heated from room temperature to 700°C at 10°C/min under nitrogen flow.

RESULTS AND DISCUSSION

The different methodologies used in this paper deal with the modification of PP with a functionalizing agent in the presence of organic peroxide. In that sense, the modification proceeds following the mechanism generally accepted for the grafting of MA or similar monomers to PP.[22,23] That is, first the homolytic scission of the organic peroxide produces radicals that abstract hydrogen atoms from the PP molecules resulting in macroradicals. Then the macroradicals follow different reaction paths, that is, molecular scission or monomer grafting. The predominance of one of these reaction paths depend on the processing conditions and concentrations.

Figure 1 displays two regions of the infrared spectra of most of the materials. The region between 1900 and 1600 cm^{-1} corresponds to the zone where the absorption bands associated to carbonyl groups are located, while the other region includes the absorption band at 1040 cm^{-1} that can be associated to the Si-O-Si groups of the clay. Each spectrum was normalized with the absorbance of the band at 2720 cm^{-1}, which corresponds to the methyne groups of the PP backbone, and arbitrarily shifted along the y-axis for legibility reasons. All the spectra correspond to purified materials as it was commented in the Section above, except the one signaled as "PPBII mixer" which corresponds to the polymer as it comes from the mixer.

It is possible to see in Figure 1 that PPp sample shows a slight intensity peak at 1720 cm^{-1}. This band can be associated to the vibration of carbonyl groups. The reactive processing in the presence of the organic peroxide might be producing some degree of oxidation, causing this small absorbance band. The spectrum of PPBII presents this absorption band and another at approximately 1740 cm^{-1}, which does not appear in either PP or PPp. The intensity of this band reduces after the purification process (compare the spectrum of "PPBII mixer" with the one of PPBII). This band corresponds to the vibration of carbonyls of the ester group, and it provides evidence of the successful grafting of BA into PP. The spectrum of PPBIII, not shown in Figure 1 for clarity reasons, presents the same absorbance band with similar intensity than in PPBII. The amount of BA grafted into PP is estimated in 0.36 wt%. This value is calculated from the ratio $A_{1740purified}/A_{1740mixer}$, being A_{1740} the absorbance at 1740 cm^{-1}, and assuming that all the BA used in the reaction (1 wt%) is present in the polymers extracted from the mixer.

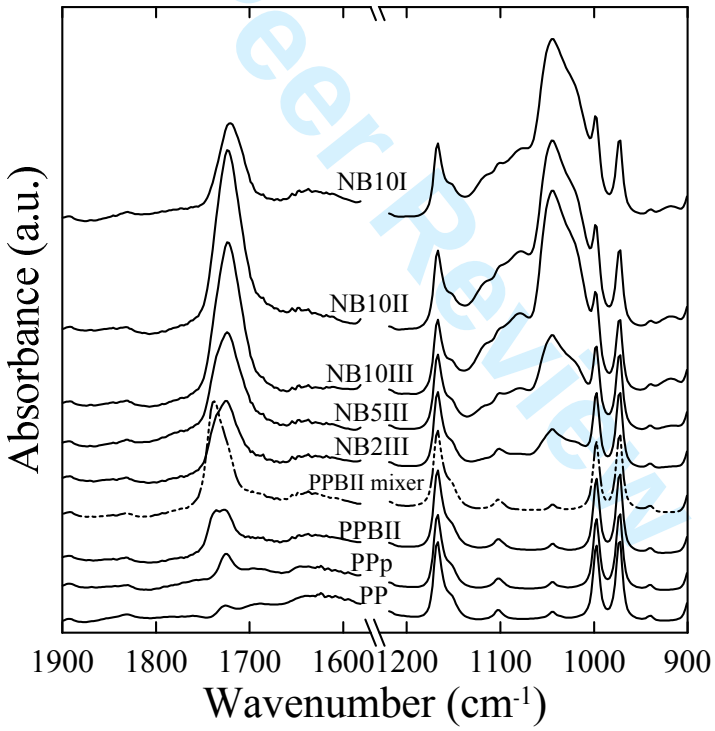

Figure 1. Regions of the FTIR spectra of PP and some of the polymers and nanocomposites.

The spectra of the composites also display a band at 1040 cm^{-1} that corresponds to the Si-O-Si groups. This band increases in intensity proportionally to clay concentration. Moreover, with the incorporation of clay, a band emerges at approximately 1720 cm^{-1}. The absorb-

ance of this band seems to be proportional to the amount of clay but it also appears to be affected by the mixing procedure. As it may be observed in Figure 1, the absorbance of the band at 1720 cm^{-1} is smaller in NB10I than in NB10II and NB10III. Moreover, in all composites, this band is larger than in the functionalized polymers. N10II and N10III also display this absorbance band, with intensity similar to NB10II and NB10III. Since the concentration of DBPH and BA used in all cases is the same, a new chemical group must be emerging during the reactive process of the nanocomposites. The new absorbance band can be associated to carbonyl groups, which might appear due to degradation of PP. This extra-degradation might be caused by the presence of oxygen introduced with the clay. In the case of Method I, the simultaneous addition of all components, reduces the degradation of PP, making less efficient the modification reaction.

With respect to the band at 1740 cm^{-1}, which corresponds to the vibration of carbonyls of ester groups, it appears as a shoulder in NB2III, and even in NB5III. The large absorbance at 1720 cm^{-1} in NB10III and NB10II might be hiding the ester band. It is interesting to notice that the 1740 cm^{-1} band is not evident in NB10I, which indicates once again that the modification reaction is less efficient in Method I. In this process, peroxide and BA are been consumed in reactions other than grafting PP.

X-ray diffraction analysis shows that the interlayer spacing of the clay, which appears at 2θ approximately 3.3 (2.6 nm), increases to 3.4-3.7 nm in the analyzed composites, regardless the mixing procedure and/or the clay concentration. Figure 2 displays the XRD patterns of the o-MMT and several composites, while Table 2 lists the values of the measured basal spacing d_{001}. The displayed diffractograms in Figure 2 are representative of at least three tested samples while the values in Table 2 correspond to the average of the d_{001} diffraction peak locations. It can be observed that the intensity of the diffraction peak corresponding to the d_{001} spacing of the clay increases with clay concentration and, within the materials with 10 wt% of clay, decreases from NB10I, to NB10II and to NB10III. Simultaneously with the smaller intensity of the diffraction peak, NB10II and NB10III display a negative slope in the smallest values of 2θ in all tested samples. The results indicate that all composites prepared in the presence of BA have similar intercalated clay structure, and that the materials processed with methods II and III have a larger degree of exfoliation and/or a fraction of clay with very large basal spacing (2θ smaller than 2°). The increase of 0.8-1.1 nm in the separation of the clay layers is a typical observation in PP nanocomposites prepared with o-MMTs similar to N44.[1,2,5,8,9]

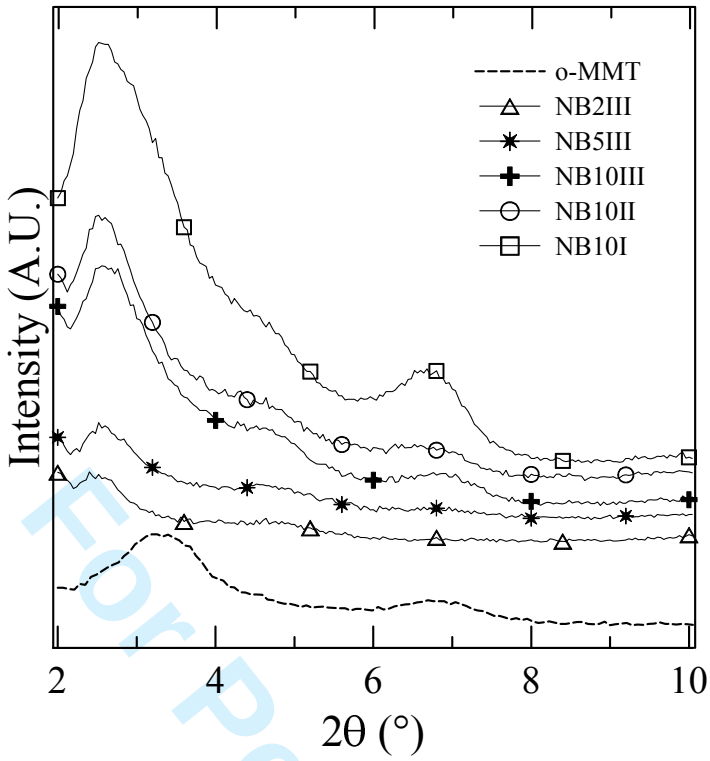

Figure 2. X-ray diffractograms of the o-MMT and some nanocomposites.

Complementing the X-ray results, Figure 3 displays three selected micrographs obtained by SEM using a magnification of 10000x. They correspond to the composites prepared with 10wt% of clay in the presence of 1wt% of BA and 0.075wt% of DBPH, using the three different mixing methods. A more detailed analysis of the morphological structure of all composites will be included in a following publication. The surfaces, which are representative of the structure observed in all composites, were obtained by cryo-ultramicrotome cut and chemically treated to enhance contrast between the clay and the polymer. The treatment consist in exposing a sample for 10 min to a solution of 0.2%v/v potassium permanganate in sulfuric acid (to slightly degrade the polymer), washing it with diluted acid sulfuric in distilled water, and finally with 20%v/v oxygenated water alternating with distilled water[8,9]. NB10III presents a homogeneous distribution of small particles and thin clay tactoids and platelets immersed in the polymer matrix. NB10II also has a homogeneous distribution of small particles and tactoids, but they are a little larger than in NB10III. In the case of NB10I, most of the clay appears in the form of small particles while practically no platelets or thin clay tactoids can be observed. The results from XRD and SEM characterization indicate that the sequential mixing technique (Method III) produces the largest amount of exfoliation of clay particles in platelets and small tactoids that are homogeneously distributed in the polymeric matrix. These conclusions are sustained by the rheological results that are analyzed in next

Section.

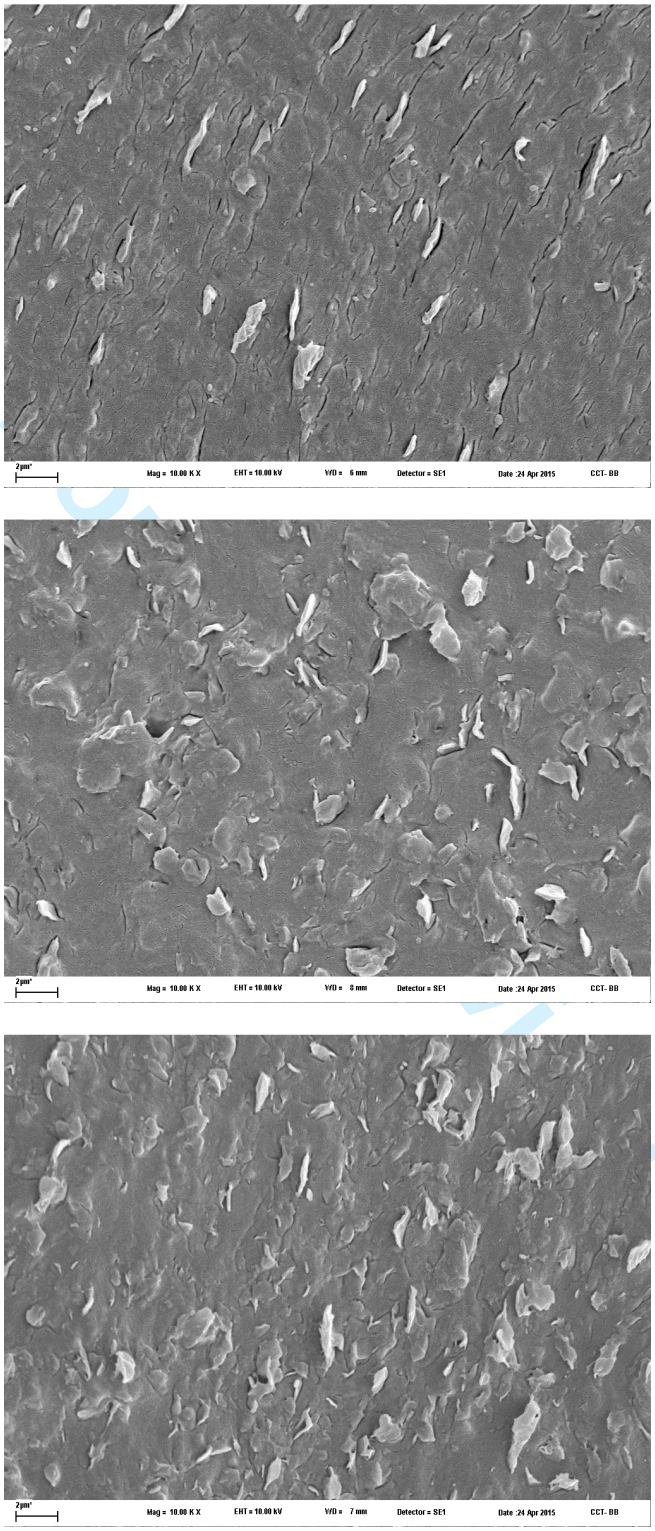

Figure 3. SEM micrographs of NB10I (top), NB10II (middle) and NB10III (bottom). Images size: 31.7 x 22.2 µm.

Rheological characterization

Figure 4 displays the elastic modulus (G′) and the dynamic viscosity (η′) of the four polymers: PP, PPp, PPBII and PPBIII, as a function of frequency. The dynamic viscosity is calculated from the viscous modulus (G″) as $\eta'=G''/\omega$. All data were obtained at 180°C. All materials have the typical rheological behavior of simple polymers. In particular, the dynamic viscosity displays a Newtonian plateau at low frequencies followed by a transition region and a final shear thinning region at higher frequencies. In the case of PPBII and PPBIII, there is a clear Newtonian plateau that extends up to large frequencies. PP has a more appreciable shear-thinning region and a less visible constant viscosity plateau. Similarly, the typical ω^2 dependency of the elastic modulus of low molecular weight simple polymers is clearly appreciated at low frequencies in the case of PPp, PPBII and PPBIII. The chain scission that occurs during the modification of PP with peroxide (PPp) produces the reduction of molecular weight that causes the observed decrease of the rheological properties with respect to those of PP. The functionalization of PP with BA in the presence of DBPH produces a material of even lower values of G´ and η´ (PPBII), which reduce even further when doubling the reaction time (PPBIII). The chain scission is more significant in these two cases, reducing substantially the molecular weight of PP. For this extra-reduction of molecular weight to occur, the concentration of radicals that attack the PP molecules must be larger in the BA-DBPH system.[23] The zero-shear-rate viscosity (η_0), which can be calculated from the value

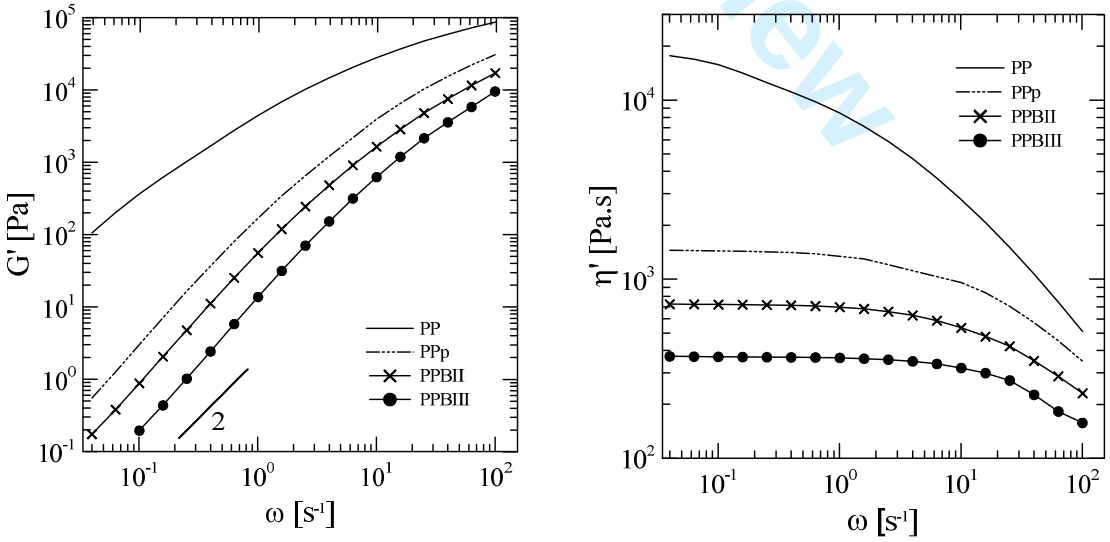

Figure 4. Elastic modulus (left) and dynamic viscosity (right) of the four polymers as a function of frequency at 180°C

of η' at small frequencies, can be used to estimate the molecular weight of these polymers. The relation $\eta_0 \sim M_w^{3.4}$, which applies to linear simple polymers,[24] gives molecular weight that are 2.3, 2.8 and 3.5 times smaller than the one of PP (330 kg/mol) for PPp, PPBII and PPBIII respectively.

Figures 5 and 6 display the dynamic moduli of nanocomposites prepared using Methods II and III, respectively, in the presence of 1wt% of BA and 0.075wt% of DBPH. The data of PP and the corresponding functionalized PP are included in each figure. The composites exhibit moduli in between those of PP and the corresponding functionalized PP. This indicates that PP has been modified in both mixing procedures, regardless the clay concentration used. In both cases, the addition of 2wt% of clay produces materials that behave practically like the PP modified with BA and DBPH, while, as expected, as the clay content increases, the dynamic moduli gradually increase, being G′ the most affected. The relative position of the curves in each figure, mainly at high frequencies, where the rheological response is dominated by the polymer matrix, suggest that the polymeric matrices in the nanocomposites prepared with Method II are similar to PPBII, while those of the composites prepared with Method III are similar to PPBIII. In that sense, the rheological results suggest that the oxidation of the polymer matrices detected by FTIR does not generate a noticeable decrease in molecular weight. Nevertheless, if the decrease in molecular weight is small, it may be concealed by the increase in rheological parameters produced by the presence of the filler.

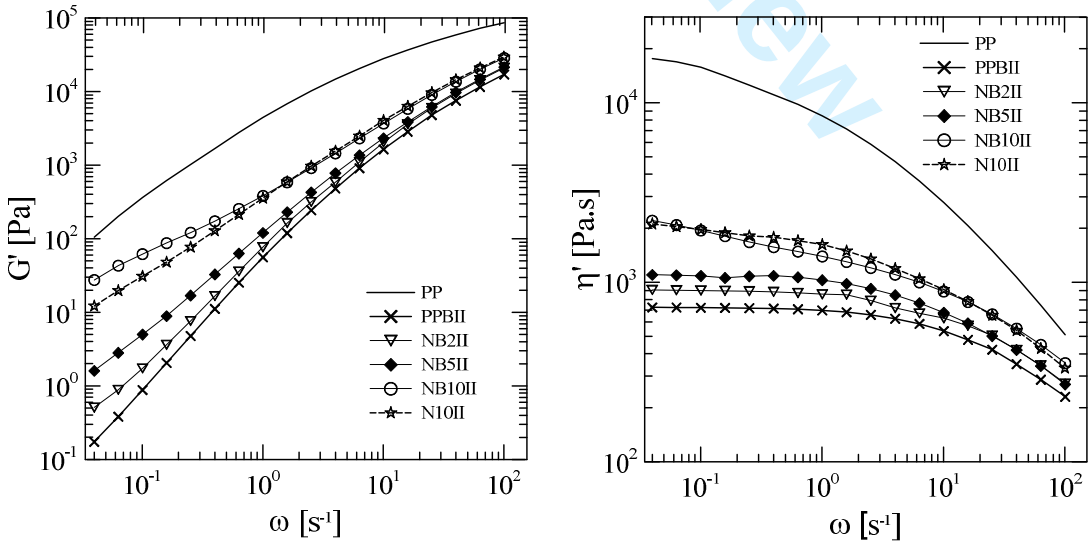

Figure 5. Elastic modulus (left) and dynamic viscosity (right) as a function of frequency of the nanocomposites prepared with different clay concentrations using Method II, at 180°C

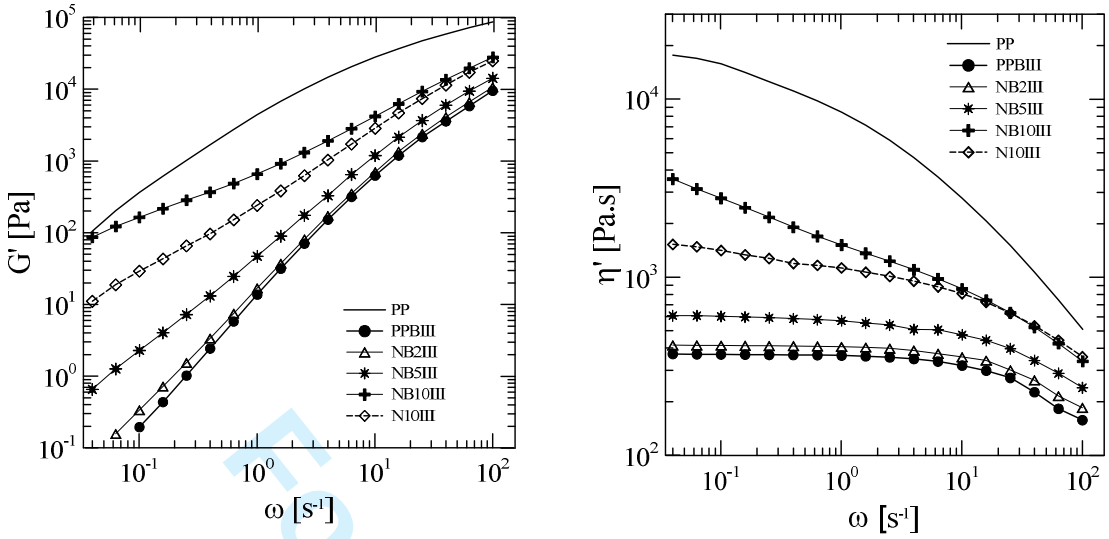

Figure 6. Elastic modulus (left) and dynamic viscosity (right) as a function of frequency of the nanocomposites prepared with different clay concentrations using Method III, at 180°C

On the other hand, the substantial change in slope of G′ (that will be further commented after Figure 7), mainly at low frequencies, both in composites prepared with Methods II and III is due to the increase in the degree of interactions among filler particles. It is well known that when a percolated filler network is obtained, a solid-like behavior is observed with a significant increase of the elastic modulus al low frequencies.[2]

Figures 5 and 6 also include the linear viscoelastic properties of N10II and N10III, respectively. These are two composites prepared with 10wt% of o-MMT in the presence of just 0.075wt% of DBPH, and no BA. Unexpectedly, at high frequencies, these two materials have moduli that are very similar to those of the composites prepared by in-situ functionalization. But, actually, this might be just a coincidence, since PPp (the PP modified with DBPH and no BA) also has rheological properties that match those of these materials (see Figure 4). At low frequencies, however, N10II and N10III have lower properties than NB10II and NB10III, respectively, indicating that the degree of delamination of the clay is lower in those composites.

Figure 7 presents the rheological properties of the composites prepared with 10wt% of clay in the presence of 1wt% of BA and 0.075wt% of DBPH, using the three different mixing methods. As a reference, the data of PP and functionalized PPs are included. In this figure it can be more clearly appreciated that the composites exhibit moduli in between those of PP

and the functionalized PPs, at least in the clay concentration and frequency ranges considered. This indicates that PP has been modified regardless of the mixing procedure used to obtain the nanocomposites. At high frequencies, the data of NB10II and NB10III practically overlap, while those of NB10I are larger. This suggest that PP has been less modified in NB10I than in both, Method II and III, and that the molecular weight of the matrix is larger in NB10I. Moreover, both G′and η′ change monotonically with ω in the case of NB10I (like in a simple polymer), signaling scarce interactions between filler particles, in spite of its large concentration, and suggesting limited exfoliation of the clay during this type of mixing procedure. This conclusion agrees with FTIR analysis, that suggests that the simultaneous mixing of the clay, polymer, peroxide and functionalizing agent (Method I) is less effective in regard to the modification of PP. Passaglia and coworkers,[17] while analyzing a propylene copolymer with low ethylene content, also found that the application of mixing methods equivalent to our Methods II and III produce a reduction of the molecular weight of the polymer (as revealed by the drop in the final torque during mixing). They also found that sequential mixing (equivalent to Method III) produces a larger reduction in molecular weight and a better dispersion of the clay particles.

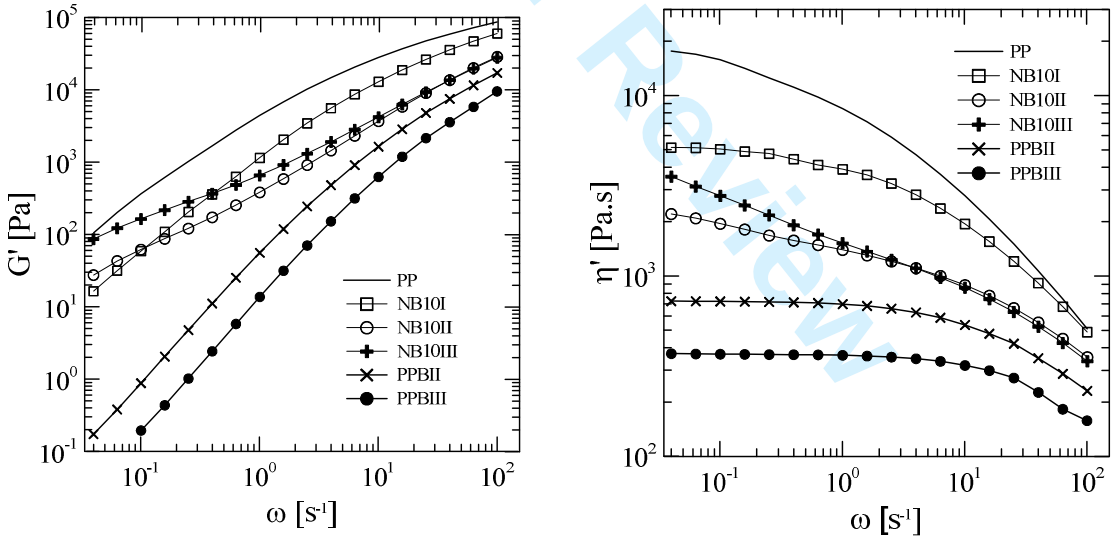

Figure 7. Elastic modulus (left) and dynamic viscosity (right) as a function of frequency of composites with 10 wt% of clay prepared by the three mixing procedures, at 180°C.

Moreover, as already mentioned, at lower frequencies, it is expected that the interaction among solid particles would produce a relative increase of the moduli, mainly of the elastic one, that would be more prominent as the exfoliation of the clay becomes more important.

According to the data in Figure 7, Method III is the procedure that promotes the largest degree of exfoliation of the o-MMT producing, nonetheless, a material with properties that are not larger than those of the original PP, at least in the considered frequency range. This is a promissory result from the processing point of view. Selecting a frequency, for example 0.04 s^{-1}, it is observed that G'_{NB10II} is ~150 times larger than the elastic modulus of PPBII and that $G'_{NB10III}$ is ~1700 times larger than G'_{PPBIII}. A similar comparison made at a larger frequency, for example at 100 s^{-1}, yields factors of approximately 1.7 and 2.8, respectively. This clearly illustrates the greater degree of interactions of solid particles in NB10III. The same conclusions can be obtained by analyzing the G′/G″ ratio, which approaches 1 at low frequencies when a material changes its behavior from liquid-like to solid-like.[2,8,9] In fact, this behavior is used as an indirect measure of the extent of delamination and dispersion of silicate layers in a polymeric matrix. In the case of NB10I, NB10II and NB10III, G′/G″ (=G′/η′ω) calculated at 0.04 s^{-1} has a value of approximately 0.07, 0.3 and 0.6, respectively.

Thermal characterization

The non-isothermal crystallization behavior of all materials was analyzed by DSC. Figure 8 displays the thermograms obtained at 10°C/min, while Table 3 lists the values of crystallization temperature (T_c) and crystallization enthalpy (ΔH_c) calculated averaging the results from three different samples of each material. T_c is obtained from the maximum of the thermograms and ΔH_c from the area of the corresponding peaks.

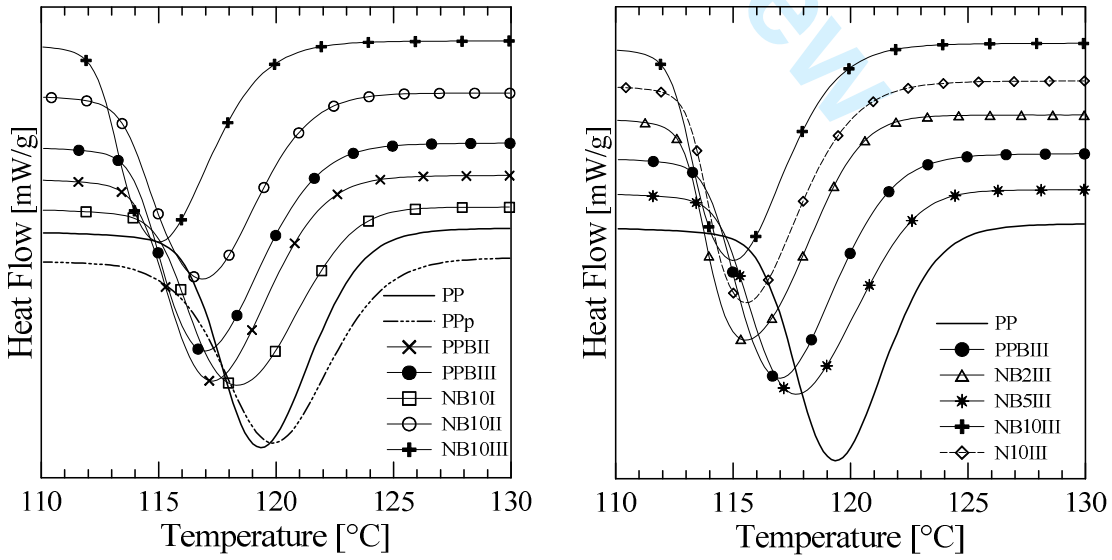

Figure 8. Exotherms of crystallization of polymers and most composites.

Table 3. Crystallization temperature and enthalpy

	T_c (°C)	ΔH_c (J/g)	T_m (°C)	ΔH_m (J/g)
PP	119	100	163	94
PPp	120	102	162	92
PPBII	117	99	161	91
PPBIII	117	100	160	90
NB10I	118	86	163	76
NB10II	117	84	161	76
N10II	115	84	160	74
NB2III	115	95	159	85
NB5III	118	92	160	81
NB10III	115	82	160	72
N10III	115	82	160	73

The crystallization of all polymeric systems occurs in about the same temperature range being the T_c of PP and PPp slightly larger than that of the rest of the materials. The crystallization enthalpy of PP, which is similar to the one of the modified PPs, decreases progressively with the addition of clay. The composites prepared with 10wt% of clay based on PP, using the different mixing procedures, present similar values of ΔH_c. These results suggest that, within the range of composition considered in this work, the clay does not produce a nucleating effect. Moreover, it rather delays the crystallization of the polymer reducing the crystallinity level. There are no crystallization studies in the literature that involve in-situ modification of PP. However, there are some studies that consider the nonisothermal crystallization behavior of PP/PPg/o-MMT systems with clay and concentration range similar to the ones used in this work.[5,6,10] They observe that the T_c of the nanocomposites is similar or slightly lower than the crystallization temperature of the PP/PPg blends. Moreover, it is generally observed that clay increases the T_c of PP,[5-7] although cases of smaller increase or practically no change have also been reported.[4-10]

Table 3 also includes the values of melting temperature (T_m) and melting enthalpy (ΔH_m) calculated averaging the results from different samples of each material. The fusion of all materials occurs in about the same temperature range and the melting enthalpy presents a behavior equivalent to the crystallization enthalpy. That is, ΔH_m of the polymer decreases with the addition of clay and reduces gradually with clay concentration, in accordance with a

reduction of crystallinity level.

The thermal behavior of the materials was completed analyzing the thermal decomposition by TGA under nitrogen flow. The evolution of the weight loss of PP, the clay and the composites with temperature is shown in Figures 9 and 10. The dried o-MMT presents two stages of weight loss, one starting at approximately 200°C associated to the degradation of the organic material, and another, not shown in the figures, above approximately 500°C, produced by the dehydroxylation of the aluminosilicates.[6,9] The 37 wt% of weight loss at about 500°C, before this second stage, is related to the concentration of intercalant in the o-MMT. In this case, it corresponds to 1.04 meq/g of inorganic clay, which, compared with the CEC value, 1.16 meq/g, signals that the modifier is in defect.[9]

The degradation of PP starts at about 320°C and ends at ~480°C. PPp, PPBII and PPBIII display the same thermal behavior than PP (not shown for clarity). With respect to the hybrid materials, they begin their weight loss at approximately 200°C and loose a small fraction of mass in an initial stage that ends at about 400°C. After that, the degradation proceeds at a faster rate than in the polymers, ending at approximately 450°C. The concentration of clay affects the initial stage of degradation and the residual mass. As the concentration of clay increases, the initial weight lost increases (see inset in Figure 9), being similar to the theoretical amount of organic material in the clay (that is, 0.7, 1.7 and 3.3wt% of the composites for 2, 4.7 and 9wt% of clay, respectively). In concordance with previous works based in the same type of clay,[2,25] this result suggests that the organic material in the clay degrades before the polymer. Moreover, the residual weight of the composites increases as the concentration of clay increases, being the values very similar to the nominal ones (that is, 1.3, 3.0 and 5.7wt% for the composites with 2, 4.7 and 9wt% of clay, respectively). All materials prepared with 10wt% of clay based on PP degrade similarly (see Figure 10), independently of the mixing procedure, that is, independently of degree of exfoliation reached by the clay and modification of PP.

With respect to the second stage of degradation (the one between 400 and 450°C approximately), it can be observed in both, Figures 9 and 10, that it is independent of clay concentration and mixing procedure. This means that all polymeric matrices degrade similarly in the presence of clay and faster than PP and the modified PPs. A factor that should be considered in this analysis is the role of the antioxidant (Irganox 1010) added to all materials at the end of their processing. This additive may slightly retard the degradation of the polymers. However, in the presence of clay, it might be absorbed by the filler and loose its protective role.

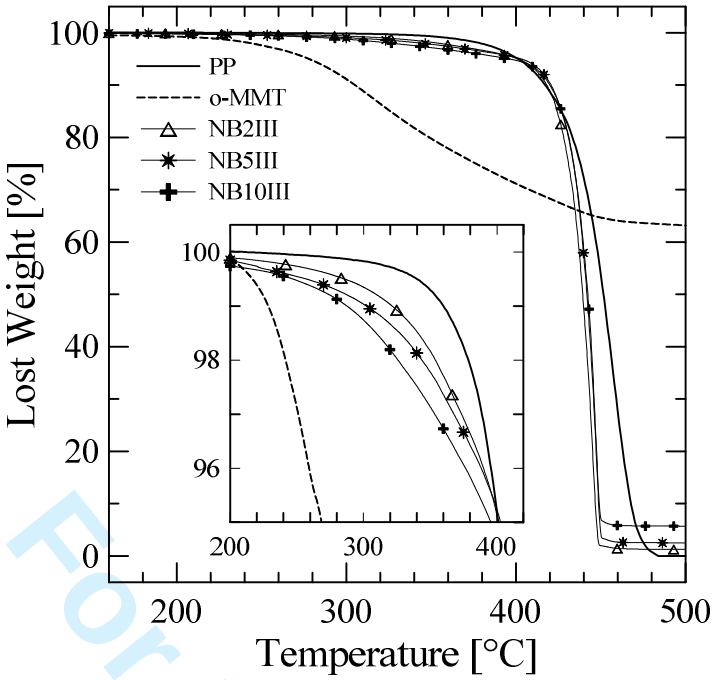

Figure 9. TGA thermograms of PP, dried o-MMT and composites prepared with Method III and different clay concentrations. Heating rate: 10°C/min

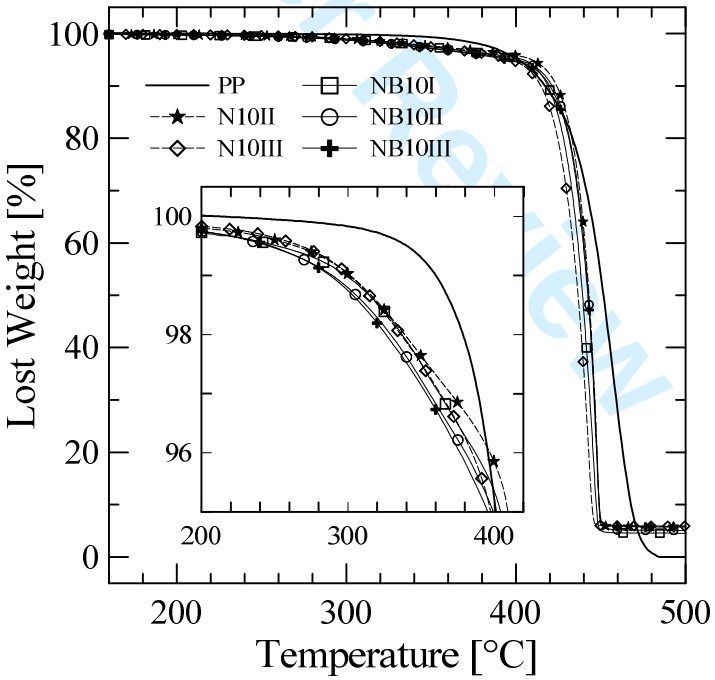

Figure 10. TGA thermograms of PP and composites based on 10wt% of clay (based on PP). Heating rate: 10°C/min.

This possibility may explain the difference in rate of degradation between polymers and composites.

Conclusions

Nanocomposites based on Polypropylene/o-MMT were prepared by in-situ functionalization of the polymer with n-butyl acrylate (BA) in one step melt reactive processing using organic peroxide as initiator. This method is a good alternative to produce PP nanocomposite at industrial level. Three procedures of mixing were considered: Method I in which all materials are simultaneously added to the mixer, Method II in which the PP is brought to the molten state and then the rest of the components are added, and Method III in which PP is melted before adding the BA and the peroxide, and mixed 20 min before the addition of the clay. The concentrations of BA and peroxide were kept constant at 1 and 0.075wt% respectively, based on PP mass, while three values of clay concentration were used: 2, 5 and 10wt%.

All methods produce the grafting of BA onto PP and composites with intercalate clay structure, being Methods II and III the ones that generate small clay tactoids. The largest degree of exfoliation of the clay was observed using Method III (the sequential method). This Method also produces the largest reduction in molecular weight. The modification of PP with peroxide produces chain scission, which increases with the functionalization with BA. The reduction in molecular weight is less significant in Method I.

However, the effect of the decrease in molecular weight on the rheological properties is somehow compensated by the interactions among the clay tactoids. These two phenomena compete and, in the range of concentrations considered in this work, they produce nanocomposites with flow properties smaller than those of PP. The largest degree of exfoliation obtained with Method III produces the largest compensation giving place to a material with dynamic properties next to those of PP when 10 wt% of clay is used. This may be advantageous for the industrial point of view since materials with improved final properties would be obtained without affecting negatively the processing conditions.

Acknowledgments

The authors are grateful for the financial support given by the National Research Council of Argentina (CONICET), the Universidad Nacional del Sur (UNS) and the Agencia Nacional de Promoción Científica y Tecnológica (ANPCyT).

References

1. Mittal, V. *Materials* **2009**, *2*, 992.
2. Sinha Ray, S. *Clay-Containing Polymer Nanocomposites: From Fundamentals to Real Applications*; Elsevier: Amsterdam, **2013**.
3. de Paiva, L.B.; Morales, A.R.; Valenzuela Díaz, F.R. *Appl. Clay. Sci.* **2008,** *42*, 8.
4. Xu, W.; Ge, M.; He, P. *J. Polym. Sci. Part B: Polym. Phys*. **2002,** *40*, 408.
5. Perrin-Sarazin, F.; Ton-That, M.-T.; Bureau, M.N.; Denault, J. *Polymer* **2005,** *46*, 11624.
6. Modesti, M.; Lorenzetti, A.; Bon, D.; Besco, S. *Polym. Degrad. Stab.* **2006,** *91,* 672.
7. Yuan, Q.; Awate, S.; Misra, R.D. *Europ. Polym. J.* **2006,** *42,* 1994.
8. Rohlmann, C.O.; Quinzani, L.M.; Failla, M.D. *Polymer* **2006,** *47*, 7795.
9. Rohlmann, C.O.; Horst, M. F.; Quinzani, L.M.; Failla, M.D. *Europ. Polym. J.* **2008,** *44*, 2749.
10. Lai, S.-M.; Chen, W.-C.; Zhu, X.S. *Composites A* **2009,** *40*, 754.
11. Zhou, R.J.; Burkhart, T. *J. Mater. Sci.* **2011,** *46*, 1228.
12. Castillo, L.A.; Barbosa, S.E.; Capiati, N.J.. *J. Appl. Polym. Sci.* **2012,** *126,* 1763.
13. Zaman, H.U.; Hun, P.D.; Khan, R.A.; Yoon, K.B. *J. Thermoplast. Compos.* **2013,** *26*, 1057.
14. Liu, M.; Guo, B.; Lei, Y.; Du, M.; Jia, D. *Appl. Surf. Sci.* **2009,** *255*, 4961.
15. Lin, Z; Huang, Z.Z.; Zhang, Y.; Mai, K.C.; Zeng, H.M. *J. Appl. Polym. Sci.* **2004**, *91*, 2443.
16. Zhang, Y.-Q., Lee, J.-H.; Rhee, J.M.; Rhee, K.Y. *Compos. Sci. Technol.* **2004,** *64*, 1383.
17. Passaglia, E.; Bertoldo, M.; Coiai, S.; Augier, S.; Savi, S.; Ciardelli, F. *Polym. Advan. Technol.* **2008, 19**, 560.
18. Borsig, E.; Lazár, M.; Hrcková, L.; Fiedlerová, A.; Kristofic, M.; Reichelt, N.; Rätzsch, M. J. *Macromol. Sci. A* **1999,** *36*, 1783.
19. Rätzsch, M.; Arnold. M.; Borsig, E.; Bucka, H.; Reichelt, N. *Prog. Polym. Sci.* **2002**, *27*, 1195.
20. Hong, H.; Jia, D.; He, H. *Front. Mater. Sci. China* **2007,** *1*, 65.
21. Sathe, S.N.; Srinivasarao, G.S.; Devi, S. *Polym. Int.* **1993,** *32*, 233.
22. De Roover, B.; Sclavons, M.; Carlier, V.; Devaux, J.; Lecras, R.; Momtaz, A. *J. Polym. Sci. A: Polym. Chem.* **1995**, *33*, 829.
23. Moad, G. *Prog. Polym. Sci.* **1999,** *24*, 81.
24. Dealy, J.M.; Wang, J. *Melt Rheology and its Applications in the Plastics Industry*, 2nd Ed.; Springer: Dordrecht, 2013.
25. Horst, M.F.; Quinzani, L.M.; Failla, M.D. *J. Thermoplast. Compos*. **2014**, *27*, 106.